Liquid Crystals
Publication details, including instructions for authors and subscription information:
http://www.informaworld.com/smpp/title~content=t713926090

The packing of azobenzene dye moieties and mesogens in polysiloxane copolymers and its impact on the opto-dielectric effect

B. Fischer; C. Thieme; T. M. Fischer; F. Kremer; T. Oge; R. Zentel

Online publication date: 29 June 2010

To cite this Article Fischer, B. , Thieme, C. , Fischer, T. M. , Kremer, F. , Oge, T. and Zentel, R.(1997) 'The packing of azobenzene dye moieties and mesogens in polysiloxane copolymers and its impact on the opto-dielectric effect', Liquid Crystals, 22: 1, 65 — 74
To link to this Article: DOI: 10.1080/026782997209694
URL: http://dx.doi.org/10.1080/026782997209694

LIQUID CRYSTALS, 1997, VOL. 22, NO. 1, 65–74

The packing of azobenzene dye moieties and mesogens in polysiloxane copolymers and its impact on the opto-dielectric effect

by B. FISCHER*, C. THIEME, T. M. FISCHER, F. KREMER, T. ÖGE† and R. ZENTEL†

Universität Leipzig, Fakultät für Physik und Geowissenschaften, Linnéstr. 5, 04103 Leipzig

†Johannes Gutenberg Universität Mainz, Fakultät für Organische Chemie, Becherweg 18–22, 55099 Mainz

(*Received 14 July 1996; accepted 22 August 1996*)

Broadband dielectric spectroscopy (10^{-2}–10^5 Hz) is used to study the opto-dielectric effect in statistical polysiloxane copolymers with side groups containing chiral mesogenic units and others containing azobenzene moieties. Below 64°C, the unexposed copolymer is ferroelectric. UV-exposure induces a photoisomerization of the azobenzene to the *cis*-configuration, and the phase transition, ferroelectric/non-ferroelectric (S_C^*/S_A), is shifted to lower temperatures. In the temperature interval between the phase transition temperatures ferroelectric/non-ferroelectric of the exposed and unexposed samples, an opto-dielectric effect is observed. The efficiency of this opto-dielectric switching depends on the packing of the chromophore within the smectic layers.

1. Introduction

Photochromic switching of molecules containing azobenzene (azo) moieties has been investigated and considered important for applications in the field of optical data storage and optical switching for more than a decade. Particular interest has been paid to the behaviour of systems containing azo moieties in a liquid crystalline (LC) matrix [1–23]. Eich *et al.* [1–5] have shown that switching from the *trans*- to the *cis*-configuration of the azo dye by UV-exposure considerably alters the phase behaviour of the liquid crystalline matrix. The contrast, non-exposed/exposed, caused in the LC matrix was used to imprint and store direct or holographic pictures in these systems [1–4, 6–7]. IR [8–10] and UV/VIS [11–15] spectroscopy were used to study the reorientation dynamics of the azo dye during exposure of the sample to polarized light. Recently azo dyes have been used as command surfaces [16–20], where the different surface alignment interactions with the liquid crystal lead to homeotropic and planar anchoring for the *trans*- and *cis*-states, respectively. Servaty *et al.* [21–23] have shown that effects similar to those described above occur in azo dye doped chiral liquid crystals with ferroelectric phases. In their measurements, the shift in phase transition temperature of the S_A/S_C^* transition gave rise to a strong opto-dielectric effect. Since the dielectric properties of ferroelectric liquid crystalline phases differ by orders of magnitude from non-ferroelectric liquid crystalline phases, the suppression of the ferroelectric phase by switching the azo-dopant to the *cis*-configuration changes the dielectric loss by a factor of 100.

Different approaches have been used in order to dope the liquid crystal with the azo-compound. Low molar mass mixtures of liquid crystals with azobenzene are the simplest, but sometimes tend to form microphase separated regions [23]. To prevent these effects, statistical side group copolymers with the mesogenic groups and azo moieties in the side groups have been used.

In this paper we describe the use of broadband dielectric spectroscopy to show the importance of an effective packing structure of the azo moieties and the mesogenic units in the side groups of a statistical side group copolymer, which is essential for the size of the opto-dielectric switching. The experimental results, the shift in phase transition temperature, and the intensity dependency of the opto-dielectric switching kinetics are consistent with a simple free energy model of T. Fischer [24].

2. Chemistry

2.1. *Synthesis of the azo dye containing copolymer*

The photoisomerizable dye **5** was chosen to carry a longer spacer than the mesogenic moiety used. The synthesis of the mesogen **7** in scheme 2 is described elsewhere [25]. The copolymer **8** investigated in this

*Author for correspondence.

0267–8292/97 $12·00

paper consists of a photoisomerizable azochromophore and a chiral mesogenic group that builds the ferroelectric matrix. It is synthesised via hydrosilylation [26] according to scheme 2. The ratio of chiral unit to chromophore is 19:1 in the monomer feed. The chromophore/mesogen ratio in the copolymer shows that there is no difference in reactivity of the two monomers (within the error of the UV-evaluation).

The phases and transition temperatures of the polymer **8**, as determined by DSC and polarizing microscopy, were found to be: S_C^* 64°C S_A 84°C I. No definite glass transition could be evaluated in DSC measurements. The system does not crystallize and shows an S_C^*- phase above room temperature.

The azochromophore **5** was synthesised in five steps according to scheme 1.

2.1.1. *4-Amino-(2-(S)-octyloxy)benzene* **1** *[27]*

The reaction is carried out under nitrogen. 3·819 g (21·93 mmol) of DEAD is added under constant stirring to a mixture of 2·396 g (30·8 mmol) of *p*-aminophenol, 2·859 g (21·95 mmol) of *S*(+)-2-octanol and 5·757 g (21·95 mmol) of triphenylphosphine in 70 ml of abs. ether. The reaction mixture is kept below −5°C during the addition and maintained at 0°C for 3 h after the addition is completed. The precipitated triphenylphosphine oxide is filtered off and the remaining solvent removed from the reaction mixture. The crude product is purified by flash chromatography on silica gel (solvent petroleum ether/ethyl acetate 3:1) and immediately used for further synthesis. Yield: 2·0 g (41·2%). ^{1}H NMR (90 MHz, $CDCl_3$): δ=0·88 (t; 3H, CH_3–$(CH_2)_5$–CH*(CH_3)–O–); 1·15–2·0 (several m; 13 H, CH_3–$(CH_2)_5$–CH*(CH_3)–O–); 3·35 (s; 2 H, NH_2–); 4·08 (m; 1 H, CH_3–$(CH_2)_5$–CH*(CH_3)–O–); 6·68 (m; 4 H, arom. H).

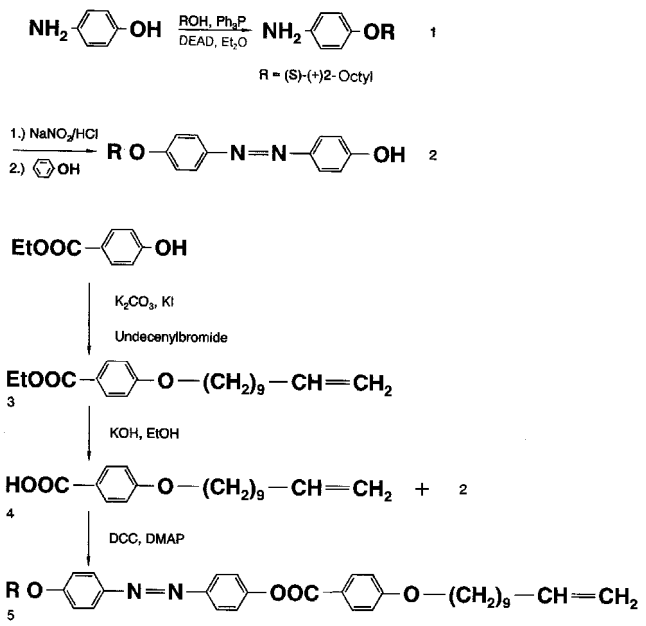

Scheme 1. Synthesis of the azobenzene chromophore.

2.1.2. *4-Hydroxy-4′(2-(S)-octyloxy)azobenzene* **2** *[28]*

1·6 g (7·23 mmol) of 4-amino-(2-(*S*)-octyloxy)benzene are added to 40 ml of 5m HCl. The temperature is held below −5°C during the addition of 3 ml of a 2·5M $NaNO_2$ solution. After the addition, more $NaNO_2$ solution is added until an iodine–starch test is positive. Urea is used to destroy superfluous nitrite. The solution is again stirred for 45 min, after which 0·7 g (7·44 mmol) of phenol dissolved in 4 ml of 2M NaOH solution are added at 5°C. During the addition the reaction mixture is kept alkaline with Na_2CO_3. Acetic acid is used to neutralize the reaction mixture after several hours of stirring at 5°C. The crude product is extracted into ether, the solvent removed and the azo dye purified further by flash chromatography (solvent petroleum ether/ethyl acetate 3:1). Yield: 1·78 g (75·2%). ^{1}H NMR (90 MHz, $CDCl_3$): δ=0·88 (t; 3H, CH_3–$(CH_2)_5$–CH*(CH_3)–O–); 1·15–2·0 (several m; 13H, CH_3–$(CH_2)_5$–CH*(CH_3)–O–); 4·43 (m; 1H, CH_3–$(CH_2)_5$–CH*(CH_3)–O–); 6·78–7·9 (several m; 8H, arom. H).

2.1.3. *Ethyl 4-(undec-10-enyloxy)benzoate* **3** *[29]*

10·0 g (60·2 mmol) of ethyl 4-hydroxybenzoate, 15·4 g (66 mmol) of 11-bromo-undec-1-ene, 20 g (66 mmol) of K_2CO_3, a catalytic amount of KI and 300 ml of 4-methylpentan-2-one are heated under reflux for 24 h. The precipitate is filtered off, the solvent removed by distillation and the pure product obtained by flash chromatography (solvent petroleum ether/ethyl acetate 6:1). Yield: 18·2 g (95%). ^{1}H NMR (90 MHz, $CDCl_3$): δ=2·1–1·2 (several m, 19 H, –$(CH_2)_8$–CH_2–O– and –COO–CH_2–CH_3); 4·0 (t, 2 H, CH_2–CH–$(CH_2)_8$–CH_2–O–); 4·4 (q, 2 H, –COO–CH_2–CH_3); 5·0 (m, 2H, CH_2–CH–); 5·8 (m, 1 H, CH_2–CH–); 6·9 (d, 2 H, arom. H); 8·0 (d, 2 H, arom. H).

2.1.4. *4-(Undec-10-enyloxy)benzoic acid* **4** *[30]*

9·11 g (28·6 mmol) of ethyl 4-(undec-10-enyloxy)benzoate in 50 ml of ethanol and 4·0 g (72 mmol) of KOH in 100 ml of ethanol are mixed and heated under reflux. After 90 min, the reaction is complete; 20 ml of water are added and the solution is brought to pH 4 with hydrochloric acid. The precipitate is filtered off and dried; recrystallization from ethanol gives the pure product. Yield: 7·8 g (87%). ^{1}H NMR (200 MHz, $CDCl_3$): δ=2·1–1·2 (several m, 16 H, –$(CH_2)_8$–CH_2–O–); 4·0 (t, 2 H, CH_2–CH–$(CH_2)_8$–CH_2–O–); 4·4 (q, 2 H, –COO–CH_2–CH_3); 5·0 (m, 2 H, CH_2–CH–); 5·8 (m, 1 H, CH_2–CH–); 6·9 (d, 2 H, arom. H); 8·0 (d, 2 H, arom. H).

2.1.5. *4-(2-(S)-Octyloxy)phenylazophenyl 4-(undec-10-enyloxy)benzoate* **5** *[31]*

0·97 g (3·08 mmol) of **2** and 1·08 g (3·7 mmol) of 4-(undec-10-enyloxy)benzoic acid are mixed in dry THF. At 0°C, 0·632 g (3·7 mmol) of dicyclohexylcarbodiimide (DCC) in 10 ml of CH_2Cl_2 containing a catalytic amount of dimethylaminopyridine (DMAP) is added dropwise. Overnight stirring completes the reaction. Following normal work-up, purification of the product is achieved by flash chromatography (solvent toluene). Yield: 1·5 g (83%). ^{1}H NMR (90 MHz, $CDCl_3$): δ=0·9 (t, 3 H, CH_3–$(CH_2)_5$–CH*(CH_3)–O–); 2·1–1·2 (several m, 29 H, CH_3–$(CH_2)_5$–CH*(CH_3)–O– and CH_2–CH–$(CH_2)_8$–CH_2–O–); 4·0 (t, 2 H, CH_2–CH–$(CH_2)_8$–CH_2–O–); 4·4 (m, 1 H, CH_3–$(CH_2)_5$–CH*(CH_3)–O–); 5·0–4·8 (m, 2 H, CH_2–CH–$(CH_2)_9$–); 5·9–5·7 (m, 1 H, CH_2–CH–$(CH_2)_9$–); 6·98 (d, 4 H, arom. H (benzoic acid); 7·33 (m, 2 H, arom. H (azobenzene)); 7·93 (t, 4 H, arom. H (azobenzene)); 8·14 (d, 2 H, arom. H (benzoic acid)).

2.1.6. *Polymer synthesis*

The copolymer **6** (see scheme 2) is obtained in a hydrosilylation reaction following the procedure given in [26]. A mixture of the monomeric alkenes in the ratio 19:1 of mesogen (**7**) to azochromophore (**5**) is used. In order to remove traces of platinum catalyst, the crude product is purified by filtration through a thin layer of aluminium oxide (90 active, neutral (grade I) by E Merck), followed by micropore filtration and repeated precipitation into methanol. The copolymer **8** obtained contains 5·0 mol % of chromophore (UV-spectroscopy) and 95·0 mol % of mesogen.

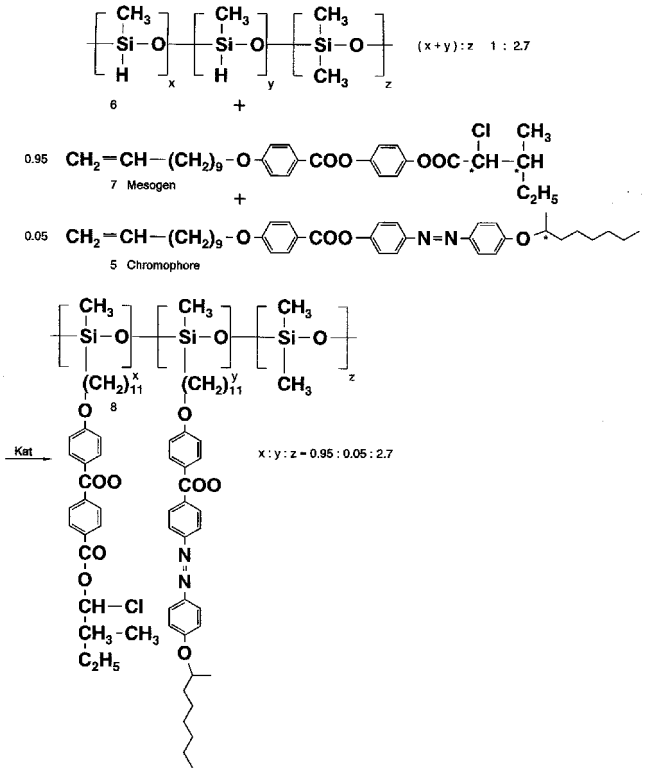

Scheme 2. Synthesis of the statistical copolymer.

2.2. *Photochemistry*

The stable configuration of azobenzene is the *trans*-configuration and this is shown in figure 1 together with the metastable *cis*-configuration. These isomeric states are separated by an energy barrier which leads to a lifetime of the *cis*-state ranging from minutes to hours. In the excited state of an azobenzene moiety, reached by the $\pi^* \leftarrow n$ transition, the equilibrium configuration lies between the *trans*- and *cis*-configuration, above the barrier of the ground state. Absorption, therefore, into the $\pi^* \leftarrow n$ transition, i.e. 365 nm from the *trans*-state and 436 nm from the *cis*-state, induces an isomerization from one state to the other with quantum efficiencies of the order of 30% [32]. The photochemical kinetics depend on the exact structure of the chromophore. The chromophore **5** of scheme 1, dissolved in chloroform has a thermal back relaxation rate (from the *cis*- to the *trans*-state) of 40 hours at room temperature, while for the dissolved chromophore used by Servaty *et al.* [23], the thermal back relaxation rate was only 14 hours at room temperature. The different photochemical behaviour of both chromophores incorporated in statistical copolymers will be discussed later in this paper.

3. Experimental

A 4 μm thick surface stabilized liquid crystalline cell with transparent indium tin oxide electrodes (EHC,

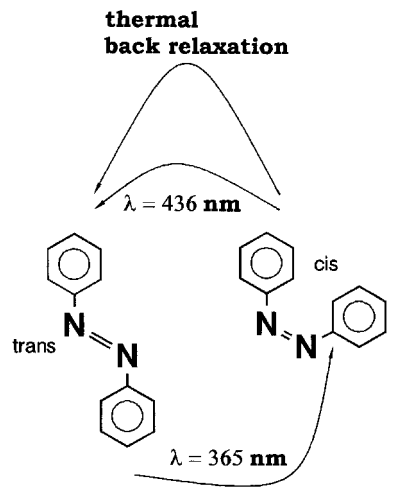

Figure 1. The two isomeric configurations of azobenzene; (*a*) the stable *trans*-state and (*b*) the metastable *cis*-state. One may switch from *trans* to *cis* with UV (λ=365 nm) and from *cis* to *trans* with visible light (λ=436 nm) or by thermal back relaxation.

Japan) is filled with the copolymer. The cell surfaces are coated with rubbed polyimide giving a planar bookshelf geometry of mesogens in the S_C^* phase. The cell is mounted in a microscope hot stage (Linkham THMS 600), which provides a temperature stability of $\pm 0{\cdot}05$ K. Proper alignment of the sample is achieved by heating and cooling, (± 5 K) across the phase transition S_C^*/S_A and by applying an electric field of 10^5 V cm^{-1}, with a frequency of 1 Hz. Once filling of the cell is completed this procedure takes about three days. Between measurements the same method is applied several times for half an hour. The alignment is generally reduced by frequency scans or light exposure measurements, and the reproducibility of the alignment reduces the accuracy of the dielectric spectra obtained. Consequently, the error in the dielectric loss is in the order of 10–20 per cent. The dielectric function is measured using a lock-in amplifier (SR 830 Scientific Instruments), in the frequency range 10^{-2}–10^5 Hz.

A Xenon high pressure lamp (XBO 101, 100 W, Zeiss Jena) is used for UV and visible exposure of the sample. An IR blocking filter (KG 1, Schott), together with a line filter (365 nm, width 12 nm and 436 nm, width 12 nm for UV and visible exposure, respectively), provides the desired wavelength. The maximum intensities reached are 0·8 mW cm^{-2} at 365 nm and 0·6 mW cm^{-2} at 436 nm.

4. Results

The chiral mesogenic moieties in the side groups of the copolymer give rise to ferroelectric behaviour. The phase sequence, measured by polarizing microscopy, is: S_C^* 64°C S_A 80°C I. Figure 2 shows the dielectric loss as a function of frequency for the unexposed sample in the S_A phase ($T=75$°C), and the S_C^* phase ($T=60$°C). One relaxation process is observed in the S_A phase. It is associated with tilt angle fluctuations of the mesogenic groups around the equilibrium orientation normal to the smectic layers. The increase of the dielectric loss towards lower frequencies is a conductivity contribution due to ionic impurities and thus will not be further discussed in this paper. In the S_C^* phase, the mesogenic side groups are tilted with respect to the layer normal and form a helical superstructure. Two relaxation processes are observed in the S_C^* phase. One is the soft-mode—a fluctuation of the tilt angle around its equilibrium value. It is covered, however, by a much stronger process, the Goldstone-mode, which originates from fluctuations of the tilt azimuth, i.e. the phase of the helical superstructure.† Due to a higher viscosity, the conductivity contribution is weaker than in the S_A phase.

Five per cent of the side groups of the statistical copolymer contain azo moieties, which are mesogenic in the *trans*-state. In the *cis*-state, however, their shape is no longer rod like and they act as strong steric perturbators of the liquid crystalline surroundings (see figure 1). Hence UV exposure of the sample, which increases the concentration of the azo moieties in the *cis*-configuration, is used to perturb the liquid crystalline phases and to shift the phase transitions towards lower temperatures. This effect is shown in figure 3, where the dielectric loss is plotted as a function of frequency at $T=60$°C for the unexposed, the UV-exposed ($\lambda=365$ nm, $I=0{\cdot}8$ W cm^{-2}) and the VIS-exposed ($\lambda=436$ nm, $I=$

† Using an additional DC field (BIAS) during the measurement unwinds the helical superstructure and suppresses the Goldstone-mode, so that the soft-mode can be seen in the S_C^* phase as well.

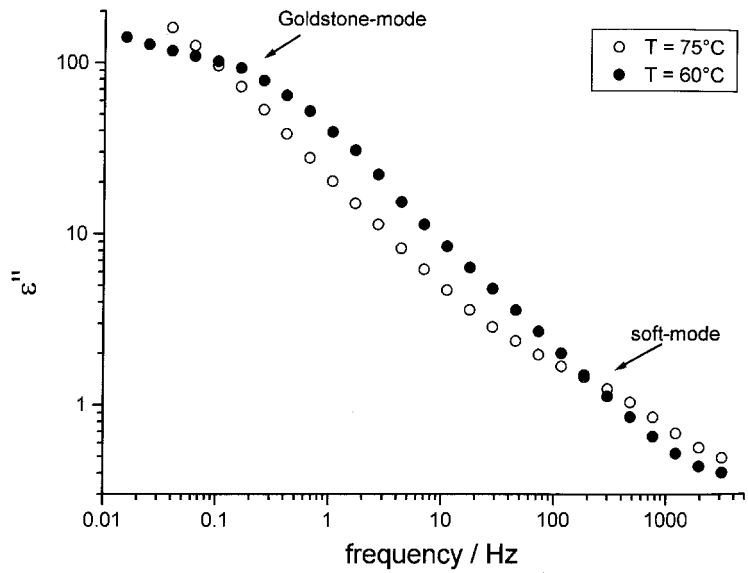

Figure 2. The dielectric loss as a function of frequency of the unexposed sample in the S_A ($T=75$°C) and the S_C^* phase ($T=60$°C).

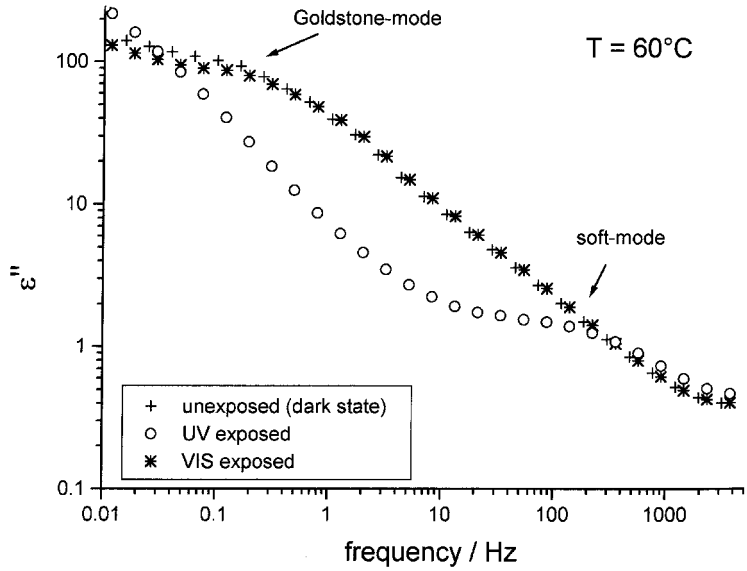

Figure 3. The dielectric loss as a function of frequency at $T=60^{\circ}C$ for the unexposed, the UV-exposed ($\lambda=365\,nm$, $I=0{\cdot}8\,W\,cm^{-2}$) and the VIS-exposed ($\lambda=436\,nm$, $I=0{\cdot}6\,W\,cm^{-2}$) states.

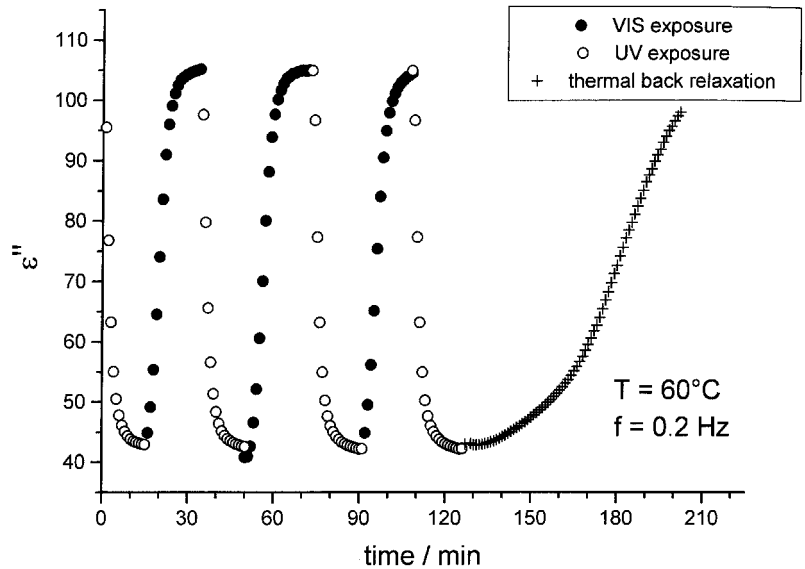

Figure 4. The dielectric loss as a function of time during exposure to UV ($\lambda=365\,nm$, $I=0{\cdot}8\,W\,cm^{-2}$) and visible light ($\lambda=436\,nm$, $I=0{\cdot}6\,W\,cm^{-2}$) for a frequency of $f=0{\cdot}2\,Hz$, demonstrating the switching kinetics. After 120 minutes the light is switched off and thermal back relaxation to the *trans*-state occurs.

$0{\cdot}6\,W\,cm^{-2}$) states. The curve of the unexposed state is the same as in figure 2 with a strong Goldstone-mode, typical of the S_C^* phase. In the UV-exposed state this relaxation process completely vanishes and the conductivity contribution together with the soft-mode remains. This proves that the UV-exposed sample is now in the S_A phase. The dielectric loss of the UV-exposed sample at $T=60^{\circ}C$ resembles the dielectric loss of the unexposed sample in the S_A phase at higher temperatures (see figure 2, $T=75^{\circ}C$). Exposure in the visible ($\lambda=436\,nm$, $I=0{\cdot}6\,W\,cm^{-2}$) switches the situation back to the dielectric loss observed for the dark (unexposed) state.

The switching kinetics that occur during exposure with UV and visible light are shown in figure 4, where the dielectric loss is depicted as a function of time at the frequency of the maximum of the Goldstone-mode in the dark state ($f=0{\cdot}2\,Hz$). UV-exposure ($\lambda=365\,nm$, $I=0{\cdot}8\,W\,cm^{-2}$) causes a strong decrease in the dielectric strength until the Goldstone-mode is completely suppressed. Exposure in the visible ($\lambda=436\,nm$, $I=0{\cdot}6\,W\,cm^{-2}$) reverses this process.‡ The optical switching is carried out several times in order to show the reproducibility of the effect. After 120 minutes the light is

‡ The saturation values in figure 4 are somewhat higher than the values in figure 3 at the corresponding frequency. This is because applying a voltage with the frequency of the Goldstone-mode as in figure 4 leads to a better alignment of the liquid crystal in the surface stabilized cell. In figure 3 the frequency is varied and the alignment of the sample is not as good as that for figure 4.

switched off and the sample returns to the dark state via thermal back relaxation. It is observed that the thermal back relaxation rate is slower than the optical switching process at the intensities used here; however, it is still of the same order of magnitude. The effects discussed above show a strong temperature dependence (figures 5 and 6). At temperatures approaching the transition temperature, S_C^*/S_A, of the UV-exposed system, the soft-mode of the exposed state becomes stronger. Accordingly, the imaginary part of the permeability at the maximum of the soft-mode can be higher than at the shoulder of the Goldstone-mode in the unexposed state at the same frequency (figure 5). Following on from this, the switching signal and kinetics at higher frequencies show at certain temperatures just the opposite effect compared to the maximum of the Goldstone-mode (figure 6).

Since the soft-mode is associated with fluctuations of the tilt angle, i.e. the order parameter of the S_C^* phase, it shows a critical slowing down at the phase transition, S_A/S_C^*. This effect can be used to measure the shift in phase transition temperature. Figure 7 gives the frequency at the maximum of the soft-mode in the S_A phase as a function of temperature for the unexposed and the UV-exposed states. The lines shown with the data are fits according to the function $f_{\text{soft-mode}} = f_0 (T - T_{AC})/T_{AC}$. The temperatures at which the frequency of these lines vanish are taken as the phase transition

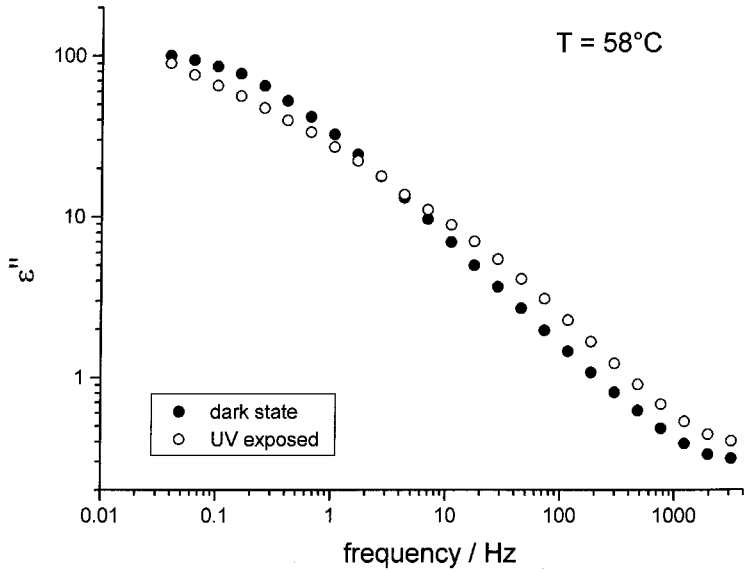

Figure 5. The dielectric loss as a function of frequency at $T = 58^\circ C$ for the unexposed and the UV-exposed ($\lambda = 365$ nm, $I = 0{\cdot}8$ W cm^{-2}) states.

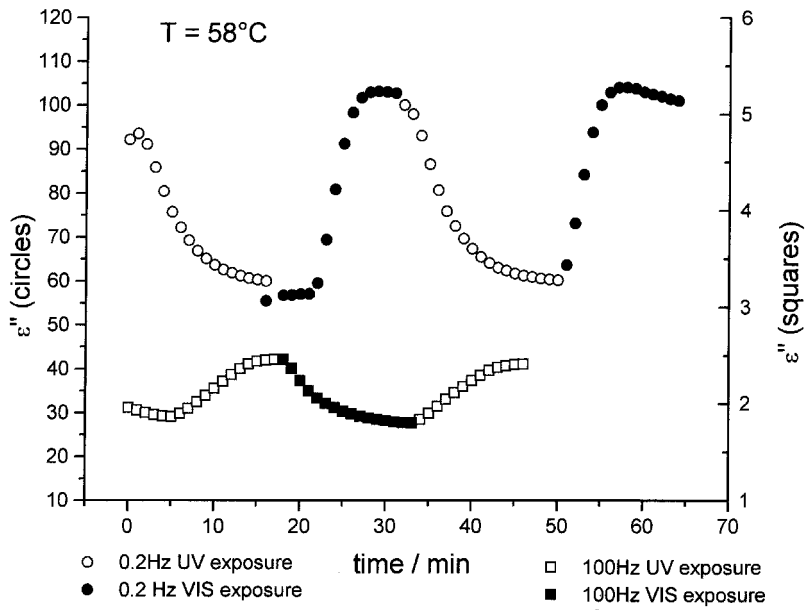

Figure 6. Switching kinetics at $T = 58^\circ C$ for two different frequencies. Dielectric loss versus time during exposure to UV ($\lambda = 365$ nm, $I = 0{\cdot}8$ W cm^{-2}) and visible ($\lambda = 436$ nm, $I = 0{\cdot}6$ W cm^{-2}) light.

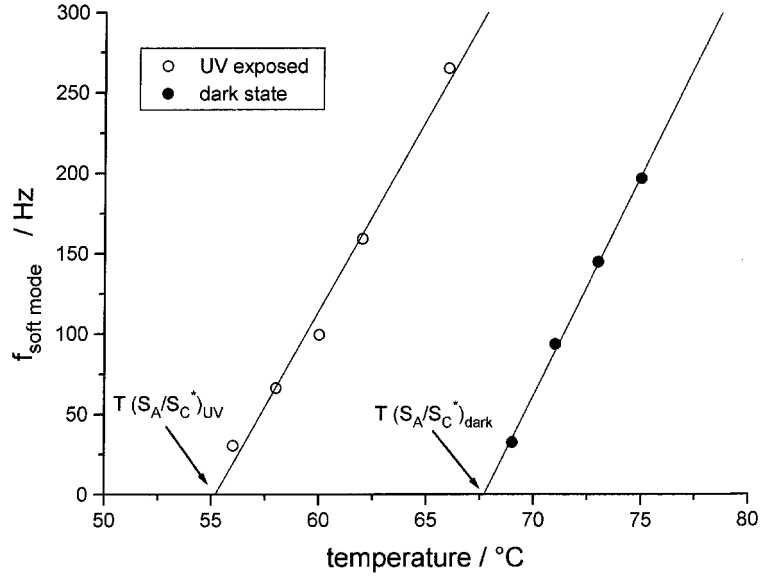

Figure 7. The frequency of the maximum of the soft-mode plotted as a function of temperature, showing the critical slowing down of the soft-mode in the dark and UV-exposed (λ= 365 nm, I=0·8 W cm^{-2}) states.

temperatures for the unexposed and UV-exposed states.§ It can be seen that there is an enormous shift in transition temperature of approximately 15 K. It is in the temperature region between the UV-exposed and the unexposed transition temperatures that the opto-dielectric effect occurs. The efficiency of the opto-dielectric effect, $(\varepsilon''_{VIS} - \varepsilon''_{UV})$, as a function of temperature, is illustrated in figure 8 for two different frequencies, 0·2 Hz (maximum of the Goldstone-mode) and 100 Hz, and for illumination intensities of 0·8 mW cm^{-2} (UV) and 0·6 mW cm^{-2} (VIS). It shows clearly that the switching is only possible in the temperature region between the transition temperatures S_C^*/S_A for the dark and the exposed states and for frequencies corresponding to the Goldstone-mode. For frequencies associated with the soft-mode, the opto-dielectric effect is weak and changes sign in the middle of the temperature interval between the transition temperatures S_C^*/S_A of the dark and the exposed states.

5. Discussion

The results from the previous section should be compared with measurements of Servaty *et al.* [21–23], who have already shown that exposure to UV leads to a suppression of the Goldstone-mode in the S_C^* phase and that switching off the light leads to its recovery (due to thermal back relaxation of the azobenzene to the *trans*-state). The copolymer they used and the one used in this paper are shown together in figure 9 and will be called copolymer B and copolymer A, respectively. The only difference is the missing benzoate group in the azo side group of copolymer B, (figure 9 (*b*)), which leads to a separation of the azo group and the main backbone chain similar in size to that of the mesogenic groups and the main chain. In copolymer A, though, the azo group is located further from the main backbone chain than are the mesogenic groups. Hence in copolymer B, the azo groups are located within the smectic layers, whereas in copolymer A they are located in the periphery of the smectic layers. This slight difference in structure causes a substantial difference in switching behaviour. While Servaty *et al.* used a UV intensity of 15 μW cm^{-2} and reached a switching time of about 100 minutes, we are unable to see an effect for copolymer A at the same intensity. We require at least 0·1 mW cm^{-2} to see any effect at all. With 0·8 mW cm^{-2} (the maximum of our Xenon lamp together with the 12 nm halfwidth filter) we reach a switching time of about 20 minutes. The back relaxation is about 50 minutes for copolymer B and 90 minutes for copolymer A.

We can understand these results by considering the structural difference which is shown schematically in figure 10. In the case of copolymer B, the switching of only a few azo groups from the *trans*- to the *cis*-state caused a strong perturbation of the highly ordered mesogenic in the S_C^* phase. Thus a very low intensity of UV was sufficient to bring the system back to the S_A phase. The interaction between the mesogenic groups and the azo side groups also altered the kinetic behaviour of the azo moieties. Because the mesogenic units have a higher free energy in the perturbed state, they feel a force which tries to drive the system back into the highly

§The phase transition temperatures obtained with this method differ from those determined with polarization microscopy by approximately 4 K, however, the phase transitions are usually smeared out in copolymers. The uncertainty of the phase transition can also be seen in figure 5, where the Goldstone-mode is not totally suppressed and some curvature in the dielectric loss remains at low frequencies, even figure 7 tells us that in the exposed state we are in the S_A phase.

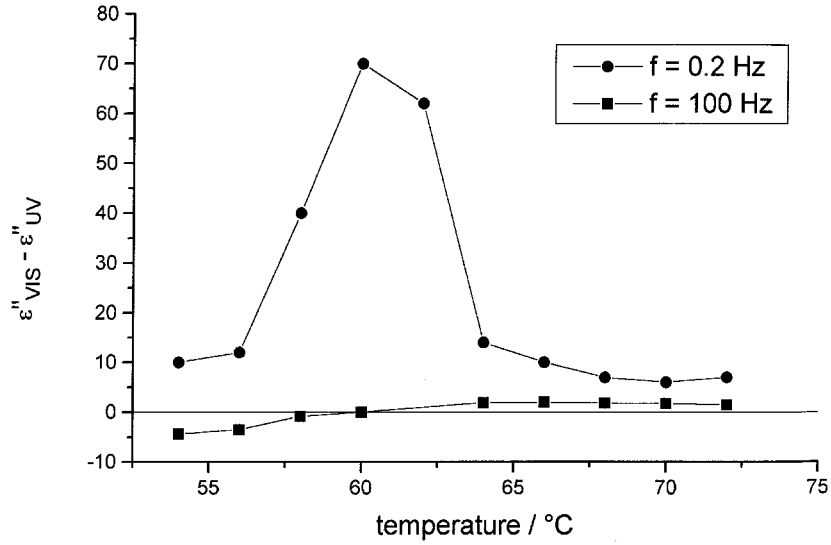

Figure 8. The efficiency of the opto-dielectric effect ($\varepsilon''_{VIS} - \varepsilon''_{UV}$) as a function of temperature for a frequency of 0·2 Hz, showing that the switching is possible only in the temperature region between the transition temperatures of the dark and the UV-exposed states.

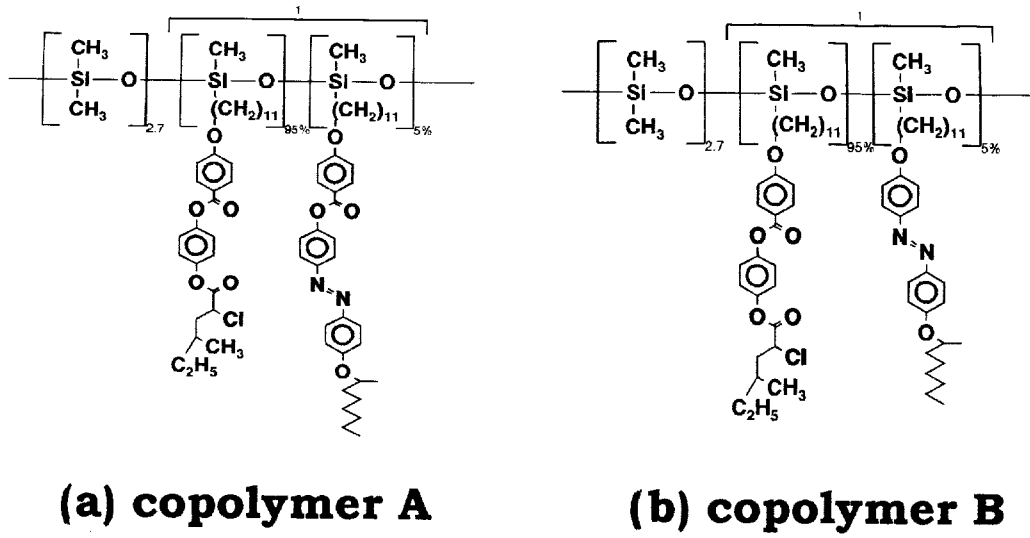

Figure 9. The statistical polysiloxane side group copolymers with azo dye moieties; (*a*) used in this paper and (*b*) used by Servaty *et al.* [23].

ordered state and the azo groups back into *trans*-state. Consequently the thermal back relaxation of the azo groups was faster in copolymer B than in copolymer A; also the measurements in copolymer B were carried out for higher viscosities, i.e. at lower temperatures due to the lower phase transition temperature.

In copolymer A, the azo group in the *cis*-state only slightly disturbs the order of the mesogenic groups, due to their far out position. Many more azo groups in the *cis*-state are therefore necessary (i.e. a much higher intensity of the UV) to drive the system into the S_A phase. The azo groups in the *cis*-state on the other side experience a smaller back driving force from the mesogenic units. The thermal back relaxation and the recovery of the Goldstone-mode are therefore slower in copolymer A than in copolymer B. T. Fischer [24] has proposed a free energy for azo doped liquid crystals including a term for interaction between the azo dye and the liquid crystalline component. He gives an expression for the shift of phase transition temperature, which depends on both the interaction strength between the azo dye and the mesogens and the intensity of the UV. At low intensities, i.e. intensities which lead to optical switching times comparable with the thermal back relaxation rate, the shift in phase transition temperature should be proportional to the intensity. For higher intensities, the shift saturates at an asymptotic value. Comparing the theory of Fischer with our experiments, we find that all experiments are carried out in the linear regime. Therefore an exposure with an intensity 50 times

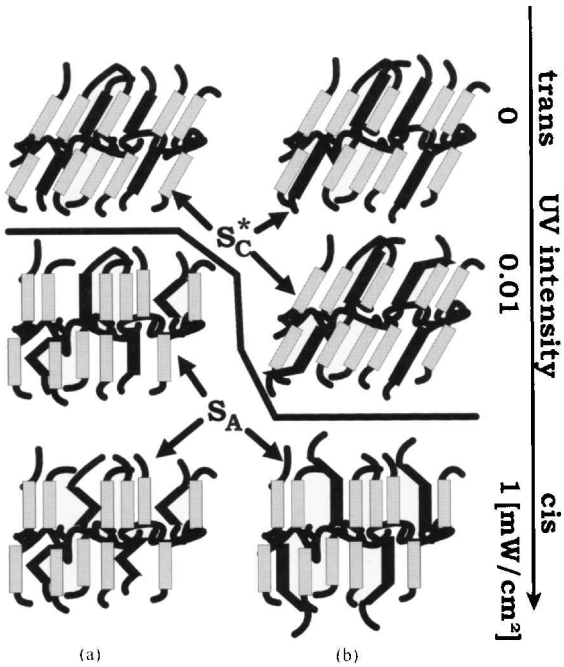

Figure 10. Schematic picture of the opto-dielectric effect caused by the steric interactions of the azo dye (black) with the mesogenic units (grey) in the sidegroups of (*a*) the copolymer B and (*b*) the copolymer A. In copolymer B the effect is stronger since the azo dye is located in the centre of the smectic layers.

smaller than 0·6 mW cm^{-2} should lead to a shift in phase transition temperature which is smaller by the same factor. The temperature region in which opto-dielectric switching is possible also shrinks by the same factor. Using the intensity of Servaty *et al.*, the temperature interval would be only 0·3 K. This is the reason why no opto-dielectric switching is observed at 60°C using the same intensity as the aforementioned. The results also suggest that the interaction strength in copolymer B is a factor 50 stronger than in copolymer A. According to Fischer's theory, it should be possible to increase the temperature range for opto-dielectric switching by further increasing the intensity. Unfortunately we as yet have no laser to enable us to make such measurements.

6. Conclusion

Broadband dielectric spectroscopy has been used to study the opto-dielectric effect in statistical polysiloxane copolymers with side groups containing chiral mesogenic units and side groups containing azobenzene moieties. Below 64°C, the copolymer is ferroelectric in the dark state. UV-exposure induces a photoisomerization of the azobenzene units to the *cis*-state and the phase transition ferroelectric/non-ferroelectric is shifted to lower temperatures. The *trans*-state of the azobenzene units and the liquid crystalline properties of the unexposed sample may be recovered by a second photoisomerization in the visible or a thermal back relaxation process. In the temperature interval between the phase transition temperatures, ferroelectric/non-ferroelectric, of the exposed and unexposed samples, the opto-dielectric effect is observed. The width of this temperature interval and the optical switching times depend on the intensity of the UV. For the polysiloxane copolymer investigated in this paper, a UV intensity of 0·8 mW cm^{-2} causes a shift in phase transition temperature of 15 K and switching times of the order of several minutes. The efficiency of the opto-dielectric switching process depends on the intensity and the packing structure of the azobenzene moieties within the smectic liquid crystalline layers. A comparison with the experiments of Servaty *et al.* [22–23] suggests that the mesogenic units and the azobenzene moieties should be equidistant from the polymer backbone in order to achieve the strongest effect. According to the theory of Fischer [24] we were using intensities where the opto-dielectric effect is proportional to the intensity. Using more intense light sources, it should be possible to induce faster switching times with an even wider temperature interval of the opto-dielectric effects.

We are grateful to Dr. J. Stumpe for many fruitful discussions. B. Fischer takes this opportunity to thank the Deutsche Forschungsgemeinschaft for providing a fellowship. This work is supported by the Deutsche Forschungsgemeinschaft under the project number Kr 1138/5-1 and by the Sonderforschungsbereich 294 *Moleküle in Wechselwirkung mit Grenzflächen.*

References

[1] Eich, M., 1987, Dissertation, Deutsches Kuststoff Institut, Darmstadt.
[2] Eich, M., Wendorff, J. H., Reck, B., and Ringsdorf, H., 1987, *Makromol. Chem. rap. Commun*, **8,** 59.
[3] Eich, M., Reck, B., Ringsdorf, H., and Wendorff, J. H., 1986, *SPIE*, **682,** 93.
[4] Eich, M., and Wendorff, J. H., 1987, *Makromol. Chem. rap. commun.*, **8,** 467.
[5] Anderle, K., Birenheide, R., Eich, M., and Wendorff, J. H., 1989, *Makromol. Chem. rap. commun.*, **10,** 477.
[6] Anderle, K., and Wendorff, J. H., 1994, *Mol. Cryst. liq. Cryst.*, **234,** 51.
[7] Ikeda, T., and Tsutsumi, O., 1995, *Science*, **268,** 1873.
[8] Wiesner, U., Antonietti, M., Boeffel, C., and Spiess, H. W., 1990, *Makromol. Chem.*, **191,** 2133.
[9] Wiesner, U., Reynolds, N., Boeffel, C., and Spiess, H. W., 1992, *Liq. Cryst.*, **11,** 251.
[10] Wiesner, U., Reynolds, N., Boeffel, C., and Spiess, H. W., 1991, *Makromol. Chem. rap. Commun.*, **12,** 457.
[11] Stumpe, J., Müller, L., Kreysig, D., Hauck, G., Koswig, H. D., Ruhmann, R., and Rübner, J., 1991, *Makromol. Chem rap. Commun.*, **12,** 81.
[12] Ivanov, S., Yakovlev, I., Kostromin, S., Shibaev, V.,

LÀSKER, L., STUMPE, J., and KREYSIG, D., 1991, *Makromol. Chem. rap. Commun.*, **12,** 709.
[13] LÀSKER, L., FISCHER, T., STUMPE, J., and RUHMANN, R., 1994, *J. Information Recording Materials*; **21,** 635.
[14] LÀSKER, L., FISCHER, T., STUMPE, J., KOSTROMIN, S., IVANOV, S., SHIBAEV, V., and RUHMANN, R., 1994, *Mol. Cryst. liq. Cryst.*, **246,** 347.
[15] FISCHER, T., LÀSKER, L., STUMPE, J., and KOSTROMIN, S. G., 1994, *J. Photochem. Photobiol. A.*, **80,** 453.
[16] SEKKAT, Z., BÜCHEL, M., ORENDI, H., MENZEL, H., and KNOLL, W., 1994, *Chem. Phys. Lett.*, **220,** 497.
[17] KNOBLOCH, H., ORENDI, H., BÜCHEL, M., SEKI, T., ITO, S., and KNOLL, W., 1994, *J. appl. Phys.*, **76,** 8212.
[18] KNOBLOCH, H., ORENDI, H., BÜCHEL, M., SEKI, T., ITO, S., and KNOLL, W., 1995, *J. appl. Phys.*, **77,** 481.
[19] SASAKI, T., IKEDA, T., and ICHIMURA, K., 1994, *J. Am. chem. Soc.*, **116,** 625.
[20] TOMITA, H., KUDO, K., and ICHIMURA, K., 1996, *Liq. Cryst.*, **20,** 171.
[21] SERVATY, S., KREMER, F., SCHÖNFELD, A., and ZENTEL, R., 1995, *Z. Phys. Chem.*, **190,** 73.
[22] SERVATY, S., KREMER, F., ÖGE, T., and ZENTEL, R., *Liq. Cryst.* (submitted).
[23] SERVATY, S., KREMER, F., ÖGE, T., and ZENTEL, R. (in preparation).
[24] FISCHER, T. (in preparation).
[25] REDMOND, M., COLES, H., WISCHERHOFF, E., and ZENTEL, R., 1993, *Ferroelectrics*, **148,** 323.
[26] HSU, C. S., and PERCEC, V., 1987, *Makromol. Chem. rap. Commun.*, **8,** 331.
[27] MITSUNOBU, O., 1981, *Synthesis*, **1,** 1.
[28] BECKER, H., DOMSCHKE, G., FANGHÀNEL, E., FISCHER, M., GEWALD, K., MAYER, R., PAVEL, D., SCHMIDT, H., and SCHWETLICK, K., *Organikum*, 1986, 16th Edn (Leipzig) pp 539, 549.
[29] CLAISEN, L., and EISLEB, O., 1913, *Liebigs Ann. Chem.*, **29,** 410.
[30] BECKER, H., DOMSCHKE, G., FANGHÀNEL, E., FISCHER, M., GEWALD, K., MAYER, R., PAVEL, D., SCHMIDT, H., and SCHWETLICK, K., *Organikum*, 1993, 19th Edn (Leipzig) pp 643.
[31] NEISES, B., and STEGLICH, W., 1978, *Angew. Chem.*, **90,** 556.
[32] RAU, H., 1988, *Photochemistry and Photophysics*, Vol. 2, edited by F. Rabek, (Boca Raton, FL: CRC Press), Chap. 4, p. 119.